Applied Thermal Engineering 167 (2020) 114805

Contents lists available at ScienceDirect

Applied Thermal Engineering

journal homepage: www.elsevier.com/locate/apthermeng

Advanced thermodynamic cycles for finite heat sources: Proposals for closed and open heat sources applications

Antonio Rovira*, Marta Muñoz, Consuelo Sánchez, Rubén Barbero

Universidad Nacional de Educación a Distancia (UNED), C/Juan del Rosal, 12, 28040 Madrid, Spain

HIGHLIGHTS

- Non-conventional cycles for closed and open finite heat sources.
- Analysis of the Hybrid Rankine-Brayton cycle considering the minimum HTF temperature.
- Proposal and analysis of the Double Expanded and Recuperated cycle.

ARTICLE INFO

Keywords:
Finite heat source
Brayton cycle
Rankine cycle
Trilateral cycle
Recompression cycle
Advanced thermodynamic cycles

ABSTRACT

This paper analyses two non-conventional thermodynamic cycles designed to work with finite heat sources, which are suitable for maximum temperatures of about 400 °C. The Hybrid Rankine-Brayton (HRB) cycle fits well to closed heat sources and, in the paper, it is analysed considering its exergy efficiency and some requirements for the maximum and minimum temperature of the heat transfer fluid that feeds the cycle, obtaining promising results. The other one is a new proposal called Recuperated and Double Expanded (RDE) cycle, aimed to translate the good features of HRB from closed heat sources to open ones, where the performance of HRB is limited.

Both cycles are compared to some reference ones. Results show that the HRB cycle is a good candidate for finite closed heat sources, particularly with maximum temperature around 400 °C and with temperature changes of the heat transfer fluid from 100 °C to 150 °C. The RDE cycle exhibits good performance for finite open heat sources with maximum temperatures between 200 °C and 400 °C, and it behaves similarly to tri-lateral cycles.

1. Introduction and background

Thermal power systems for electricity production based on renewable energies or on waste heat recovery will involve technologies that must cope with certain limitations in the temperature of the heat source. Among the different technologies, solar thermal power plants (STPP) fed by a heat transfer fluid (HTF), geothermal systems fed by brines and plants based in heat recovery from renewable or waste energy will play an important role in the future.

As it is known, when the heat source is finite, the heat transfer requires a change in the temperature of the HTF. These finite sources can be categorised into two groups, namely closed and open heat sources [1], which may present some differences in the temperature variation requirements.

For example, in STPPs (closed heat sources), the HTF that feeds the heater of the thermodynamic cycle is sent back to the solar field, so its residual thermal energy is not wasted. Furthermore, its temperature at this point is usually constrained (for example, due to limitations of the fluid, or due to the thermal storage system design or even because of the thermodynamic optimization). Therefore, the HTF works in a well-defined range of temperatures, between a maximum temperature that depends on several factors (among them the fluid characteristics) and a minimum temperature, with the limitations mentioned above.

On the other side, in heat recovery systems (open heat sources), the residual thermal energy of the heat carrier is lost (i.e. the exhaust gas of a gas turbine or geothermal brines unless the reinjection to the well has a significant contribution to the ground temperature [1]), so the HTF temperature at the exit of the heat recovery system must be as low as possible (although, in practise, there is some weak limitation, for example, to avoid the acid dew point in the equipment or mineral precipitation in brines).

In the technical literature there are many works focused on the use

* Corresponding author.
E-mail addresses: rovira@ind.uned.es (A. Rovira), mmunoz@ind.uned.es (M. Muñoz), csanchez@ind.uned.es (C. Sánchez), rbarbero@ind.uned.es (R. Barbero).

https://doi.org/10.1016/j.applthermaleng.2019.114805
Received 28 May 2019; Received in revised form 22 November 2019; Accepted 15 December 2019
Available online 16 December 2019

Nomenclature

Symbols

c_p	specific heat at constant pressure (J kg^{-1} K^{-1})
DRDE	double recuperated and double expanded
HTF	heat transfer fluid
HRB	hybrid Rankine-Brayton
HRSG	heat recovery steam generator
$\dot{m}$	mass flow rate (kg s^{-1})
ORC	organic Rankine cycle
r	pressure ratio (–)
RDE	recuperated and double expanded
s	entropy (J kg^{-1} K^{-1})
STPP	solar thermal power plant
T	temperature (K)
tORC	transcritical organic Rankine cycle
w	specific work (J kg^{-1})
$\dot{W}$	power (W)
x	Mass fraction (–)
2P	dual pressure level
3PR	TRIPLE pressure level with reheat

Greek letters

η	Efficiency, thermal efficiency (–)
η_ε	exergy efficiency (–)

Subscripts

bal	balancing
C	compressor
max	maximum
min	minimum
P	pump
sec	secondary
T	turbine

and management of low to medium grade finite thermal sources [2–4]. Organic Rankine Cycles (ORCs), either subcritical or transcritical, are considered a good solution for such applications with limited power rate [5,6] as they are implemented in smaller and simpler facilities than conventional steam cycles, because the densities of the organic fluids are high and the use of extraction lines from the turbine is avoided. The maximum temperature in ORCs ranges from 80 °C to 400 °C. They have been proposed for concentrating [7,8] and non-concentrating [9] solar power plants, biomass, geothermal systems [10] and high grade waste heat recovery [11,12] (including the exhaust gas of gas turbines in combined cycles and internal combustion engines) and even as alternatives for low grade heat recovery, such as the Misselhorn cycle [13,14].

There are also works that study or propose Brayton cycles for low or moderate maximum temperatures [15,16], which are also simpler than conventional Rankine cycles and can work with unattended operation, but their efficiency is usually low at the considered range of temperature. In fact, to achieve a more competitive efficiency, the maximum temperature required from the source should be extended from about 400 °C to 1000 °C. For that reason, they usually are proposed for high concentrating solar power systems [17,18] and for waste energy recovery [19].

Another option for Brayton cycles is the use CO_2, for example, for solar applications [3,7,20]. Recently, great attention has been put on the use of supercritical CO_2 (sCO_2) cycles, particularly the re-compression cycle or Feher cycle, which includes two compressors and two recuperators [21,22]. The maximum temperature range advisable for this cycle is moderate-to-high, ranging from 500 °C to 1000 °C, and it has been proposed mainly for high concentrating solar power [23–26], nuclear power plants [27,28], high grade waste heat recovery systems [29], and even geothermal and fuel cells [30].

There are other proposals of non-conventional thermodynamic cycles [3,31,32] and cycles combining several heat sources with different temperature requirements in only one system [33], integrating geothermal and concentrating solar power [34,35], waste and solar energy [36] or solar and biomass [37,38].

Particularly, Rovira et al. [39] proposed a non-conventional thermodynamic power cycle for applications of moderate heat source temperatures (below 500 °C), that was referred as Hybrid Rankine-Brayton (HRB) cycle with balanced recuperator (B-HRB). Among other favourable characteristics, this cycle allows constant temperature heat rejection and low irreversibility in the heat exchangers, especially in the recuperator, which is well balanced, and it may lead to high efficiencies. The cycle works at supercritical pressure, while other solutions aiming similar features have been proposed for sub-critical working pressures [40].

In Ref. [39], the proposed HRB cycle was compared with other conventional and non-conventional thermodynamic cycles, among them, sCO_2, ORCs and regenerative steam Rankine cycles. That study was a preliminary conceptual approach for the application to solar power plants but with no reference to any plant site that may determine operational aspects. Instead, a thermodynamic optimization was performed to investigate the maximum efficiency achievable, considering some boundary conditions, namely, the ratio of maximum temperature of the heat source to minimum temperature of the heat sink (equal to 2.2) and a fixed variation (100 °C) in the HTF temperature along the heater. The results showed that the balanced HRB cycle achieved higher efficiency than sCO_2 cycles and ORCs, and similar to steam Rankine cycles, but with a remarkable advantage of simplicity, as it employs a single recuperative heat exchanger rather than several extraction lines from the turbine and the corresponding preheaters.

In Ref. [41], another step was taken in the definition and analysis of the HRB cycle, studying its performance at off-design operation in the particular case of a Solar Thermal Power Plant (STPP) that receives the heat source from a solar field of parabolic trough collectors, with a maximum temperature of the heat carrier (oil in that case) of 395 °C, and evaluating the annual performance in a particular site (Almeria). Also, the work compares different possible working fluids, among which propane stood up as a good option. As a conclusion, the HRB showed its potential as a good alternative for finite close heat sources working at moderate temperatures, up to 400 °C.

The key aspect of the research line is the development of non-conventional thermodynamic cycles conveying high efficiency. HRB cycle was proposed for pure STPP plants, obtaining promising results, but its extension to hybrid power plants with heat recovery was not successful due to the different nature of the heat source: while STPP uses a closed heat source, heat recovery from hybrid systems is an open one. Thus, some modifications to the HRB cycle were done resulting in the RDE cycle.

In the paper, the suitability of both cycles is studied for a range of temperatures typical for conventional solar collectors and exhaust gases. It is emphasized that the type of source has a decisive impact on the type of cycle to be used and its optimization.

To that aim, in the first stage, a parametric study was carried out to evaluate the influence of three main design parameters of the HRB cycle, namely maximum heat source temperature, pressure ratio and balancing mass flow fraction, comparing its behaviour with that of two other types of thermodynamic cycles: Steam Rankine and ORCs,

working with identical values of maximum heat source and minimum heat sink temperatures. The analysis also studies the value of the minimum temperature of the HTF (differing this approach from that followed in previous works [39]). This allows identify the HRB cycle as a very good candidate when minimum temperature for the HTF is moderate (typical of closed heat sources) but, on the contrary, the cycle is not adequate to work with open heat sources that imply low HTF temperatures at the exit of the heat recovery system (in the range of 100 °C). Thus, some modifications are required, as it will be latter explained, which leads to the proposal of another configuration, named Recuperative and Double Expanded (RDE) cycle.

Therefore, another objective of the paper is the introduction and a first evaluation of this second configuration, more appropriate for open heat sources, at a determined range of temperatures. This proposal preserves the main features of the HRB cycle: heat rejection at constant temperature and low irreversibility in the heat exchangers, with balanced recuperator (as it will be explained) but it is optimised to enlarge the heat recovery from the heat source.

Since the technological readiness level of both cycles (HRB and RDE) is low, the study is not focused in a determined power rate or in the detailed analysis of a power plant for a specific use and site. As mentioned, the work aims to study these unconventional cycles in a certain range of temperatures, at which they can convey some advantages over other solutions, and it is done regardless the power rates. Among their possible uses, stand out concentrating solar power systems (closed sources) and solar hybrid plants (open sources using heat recovery form a fossil or biomass application, for example). Power rates of these applications can go from a few MW (i.e. 20 MW to 200 MW), so conventional ORCs and dual and triple HRSG are possible competitors.

This fact limits the analysis to the use of figures of merit that do not depend on the size or power rates. Also, yearly operation and economic aspects are out of the scope of this work.

Sections 2 and 3 present the configurations proposed for the two types of sources: HRB for closed heat sources and RDE for open heat sources. The reference cycles that are introduced for comparative purposes are also presented in these respective sections. The methodology and simulation models are presented in Section 4. The main results of the analysis of the HRB performance under different design scenarios, that led to the proposal of the RDE configuration, are shown in Section 5.1. Section 5.2 present the analysis of the RDE cycle. The suitability of both cycles is studied for a range of temperatures typical for conventional solar collectors and exhaust gases, each one using the respective type of heat source and with a maximum cycle temperature up to 400 °C. The main conclusions are summarized in Section 6.

2. Closed heat source applications: HRB cycle

Closed heat sources [1] work with HTF having a well-defined maximum and minimum temperatures. The HTF is heated up to the maximum allowed temperature by the heat source. Then, it is sent to the heater of the thermodynamic cycle, where it transfers its thermal power to the working fluid of the cycle. Finally, it is sent back to the heat source at a well-defined return temperature. The HTF temperature change selected at design conditions (usually kept nearly constant at off-design operation) depends on various factors, some of them related to the optimization of the thermodynamic cycle (efficiency increases as the mean heating temperature increases), the heat source features (for example, thermal efficiency of solar collectors is dependent on HTF average temperature), the thermal storage system design and on the properties of the HTF (for example, crystallisation of a molten salt), that in turn impose certain limitation in the adequate minimum temperature of the HTF.

The HRB cycle [39,41] is proposed for the case of closed heat sources with fixed temperature change and a maximum temperature of the heat source up to 400 °C. The cycle is shown in Fig. 1 and its temperature-entropy diagram in Fig. 2.

HRB cycle consists of two thermo-hydraulic circuits partially integrated, one of them following a transcritical Rankine cycle and the other following a Brayton cycle, in such a way that the complete cycle is composed of a Rankine cycle coupled in parallel to a Brayton cycle. The heating process and the fluid expansion are common for both integrating cycles, so they take place in the same equipment and there are only a heater and a turbine. However, the compressor of the Brayton cycle bypasses the condensing and pumping processes of the Rankine cycle. The HRB cycle includes a recuperator in which the total stream that comes from the turbine outlet heats up the mass flow fraction coming from the pump. This fraction is mixed at the exit of the recuperator with the other fraction that comes from the compressor.

As it was commented in Ref. [39], selection of the mass flow fraction that goes through the compressor is a critical aspect. Provided that the specific heat of the liquid fluid is higher than that of the vapour, a possible criterion is to equal the heat capacities of both the hot and cold streams in the recuperator, so the product $\dot{m}\cdot c_p$ is the same for both streams, liquid and vapour. This selection makes the recuperator well balanced, which leads to low irreversibility in the recuperator. For that reason, the mass flow fraction to the compressor was called balancing mass fraction in this previous work. This idealized solution is the best one if all the components have not any irreversibility, although real inefficiencies in the different equipment can modify the optimal balancing mass fraction and its value should be analysed in each design.

To consider the balancing mass flow fraction (x_{bal}) as a design parameter of the system, it can be defined as below:

$$x_{bal} = \dot{m}_{bal}/\dot{m}_{heater} \quad (1)$$

where $\dot{m}_{heater}$ is the total mass flow that is heated by the heat source.

The maximum and minimum working fluid temperatures are specified, the latter corresponding to nominal ambient condition of 25 °C plus 10 °C. Once the temperatures, the fluid and the balancing mass flow rate have been defined, the main design parameter of the cycle is the pressure ratio, which relates the heating pressure to the cooling one.

Fluid selection is a key issue to guarantee that the special characteristics of the HRB cycle are preserved (even at off-design conditions): ensuring a supercritical heating pressure, condensation of the working fluid in the heat sink and a compression process of the bypass

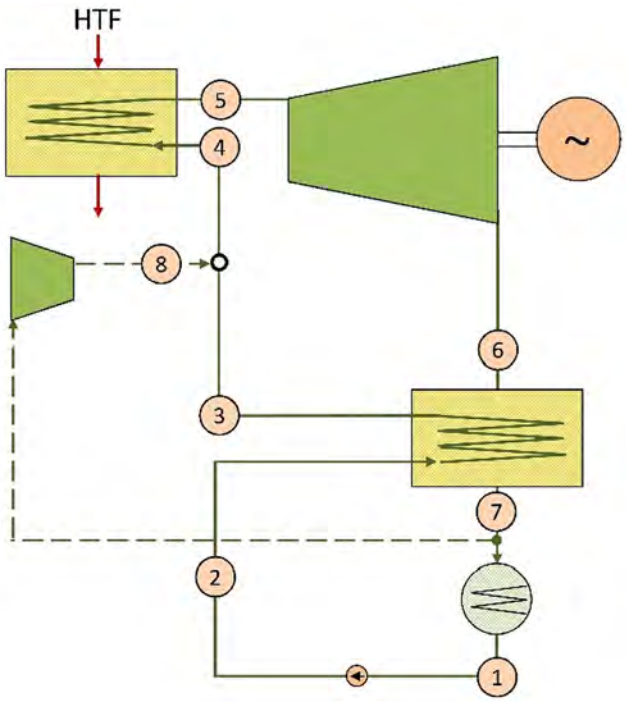

Fig. 1. Layout of the HRB cycle.

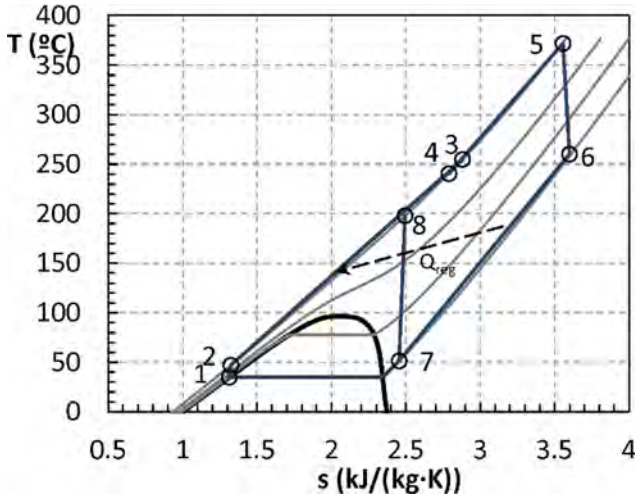

Fig. 2. Temperature-entropy diagram of the HRB cycle.

flow well away from the two-phase region to avoid wet compression. On the other hand, operation at high temperature may cause the working fluid degradation.

As it was studied previously [41], propane is a good candidate for the cycle due to its good performance, the low pressure ratio required in the compressor and its chemical stability for the maximum temperature of the heat source considered. Thermal-physical properties are taken from Lemmon et al. [42].

The reference cycles that allow the comparison of the proposed ones are two. Given the range of working temperatures (up to 400 °C), conventional steam Rankine cycles are probably not the best solution due to the complexity of the facilities, but these cycles can provide high thermal efficiency and its comparison could be considered mandatory. Water steam properties are taken from the IAPWS formulation [43]. To approach a realistic Rankine cycle, five regenerative preheaters are included, which are fed by steam extraction lines from the turbine placed at constant enthalpy variation along the expansion (Fig. 3).

On the other side, recuperative ORCs (Fig. 4) are also selected for comparative purposes as they are cycles simpler than conventional Rankine ones that are being considered for these kinds of applications. The selected fluids for ORCs are toluene and ethanol, which can be used at the proposed range of temperatures. The first one is one of the best fluids for ORC due to its high critical temperature and high heat capacity of the vapour (the influence of the specific heat of the vapour is analysed, for example, in [6]). On the other hand, the use of ethanol allows the comparison of a transcritical Rankine cycle, and it is a good candidate due to its high critical temperature. Their properties are taken from Lemmon and Span [44] and Dillon and Penoncello [45] and the ranges of applicability specified in relation to the maximum temperatures (426 °C for toluene and 377 °C for ethanol) fit well to the maximum temperature fixed in this work.

3. Heat recovery applications: RDE cycle

Open heat sources should be designed to recover as much thermal energy as possible, reducing the exhaust temperature of the HTF at maximum. As in the previous case, the heat source heats the HTF up to the maximum temperature. Then, it is sent to the heater of the thermodynamic cycle. Finally, the it is wasted to the environment at low temperature (eventually limited by the acid dew point or mineral precipitation).

The cycle proposed for these applications is based on the HRB cycle, but several modifications are introduced. Firstly, as it is depicted in Fig. 5a, the compressor is removed, and a secondary expander is included instead. Secondly, the condensed flow is divided into two streams after it is pumped. The main one goes to the heater and the secondary one is directed to a recuperator that is fed by the vapour exiting from the main expander. The temperature-entropy diagram is represented in Fig. 6a. Due to the existence of the recuperative process and two expansion processes the cycle is named Recuperated and Double Expanded (RDE) cycle.

Even, a secondary recuperator could be included to preheat the main stream using the vapour exiting the secondary expander before it enters in the heater (Figs. 5b and 6b), configuring a double recuperated and double expanded cycle (DRDE).

Thus, the cycle contains two heating lines, the main one that is heated by the heat source (this line can be slightly pre-heated by the secondary stream in case of including a secondary recuperator, DRDE configuration), which allows a high heat recovery from the heat source; and a secondary line, which is strongly heated within the recuperator by the vapour coming from the main expander. As the fluid at the exit of this recuperator is at supercritical state, a secondary expander is introduced to increase the mechanical power, which increases the energy conversion.

A fluid that fits well to this cycle is, again, propane. For the same reasons as previously, the maximum considered temperature is 400 °C.

The mass flow rate of the secondary stream can be determined using a secondary mass fraction, defined as the ratio of the secondary mass flow rate to the main mass flow rate (which is heated by the heat source):

$$x_{sec} = \dot{m}_{sec}/\dot{m}_{heater} \quad (2)$$

The total mass flow rate that is condensed and pumped is the sum of both streams, main and secondary ones. Again, a possible criterion to select this secondary mass fraction is to balance the secondary recuperator, making the $\dot{m}\cdot c_p$ equal for both streams (vapour coming from the main expander and secondary stream coming from the pump).

Once the maximum and minimum temperatures, the fluid and the secondary mass flow rate are defined (whatever the criterion), the main design parameter of the RDE cycle to be selected is the pressure ratio.

In this case, the reference cycles that allow the comparative evaluation of the proposed one are steam cycles fed by dual (2P) and triple pressure (3P + R) level heat recovery steam generators (HRSG), largely used in combined cycles (Fig. 7). As it is usual in combined cycles, the 3P + R includes steam reheating at the intermediate pressure level. The RDE cycle is also compared to simpler facilities consisting in ORC (see Fig. 4) using ethanol, R11 (properties from Jacobsen et al. [46] with range of applicability of the correlations up to 377 °C), propane and

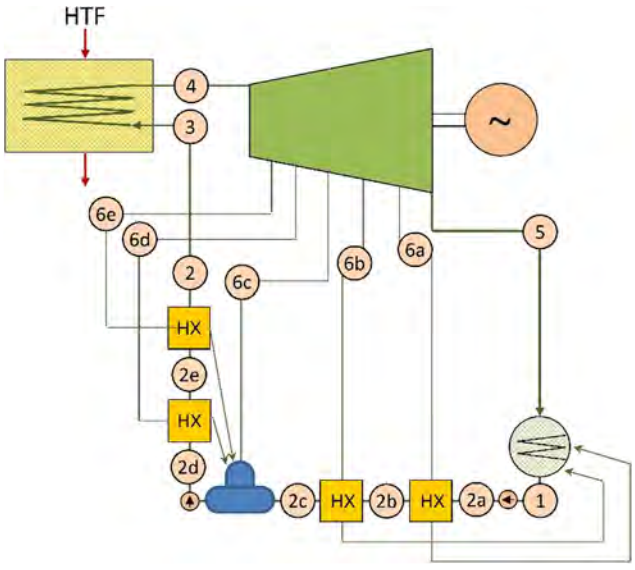

Fig. 3. Layout of a Steam Rankine cycle with five regenerative pre-heaters.

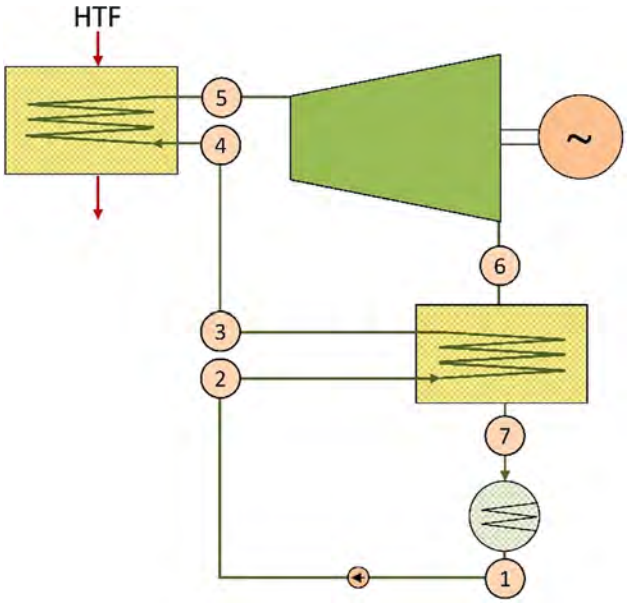

Fig. 4. Layout of a recuperative Organic Rankine Cycle.

toluene. Beyond the specified temperature limits, the correlations have not been verified, and chemical stability has not been confirmed. The two first fluids (ethanol and R11) configure quasi-triangular transcritical ORCs or trilateral cycles [1,32] that should lead to quite good performance. Transcritical ORC using propane and subcritical ORC using toluene are also analysed for comparative purposes.

4. Methodology

4.1. Boundary conditions

In all cases, two scenarios for the heat source are considered. Firstly, The HTF is assumed to operate at a maximum temperature of 400 °C (typical of a parabolic trough solar thermal power plant). In this scenario and for the cases of closed heat sources, the minimum temperature is set to 290 °C, while the exiting HTF temperature is a result for the open heat source cases.

The maximum temperature of the working fluid of the thermodynamic cycles is as high as possible considering a pinch point in the heater of 5 °C [47], unless this temperature exceeds the limit that impose correlations used to determine the properties of the fluid (see Table 1).

Secondly, to analyse the suitability of the proposed cycles at lower heat source temperatures, the first scenario was varied, and the analyses were repeated reducing the maximum and minimum HTF temperatures 100 °C. Thus, the second scenario considers a maximum HTF temperature of 300 °C. In the cases of closed heat sources, the minimum temperature is also modified and set to 190 °C.

Ambient temperature is always set to 25 °C and the condensation temperature to 35 °C, corresponding to different condensation pressures depending on the working fluid of the thermodynamic cycle (Table 1). In the case of propane, the condensation pressure takes a value of 12.2 bar, which is well above the ambient pressure.

4.2. Processes simulation

The thermodynamic cycles consist, basically, in a concatenation of processes that can be classified into polytropic ones, heat transfer ones and processes of stream splitting and mixture. For all the processes the mass and energy balances must be accomplished.

The energy balances of equipment different from turbomachinery can be calculated with the following equation:

$$\sum_{inlet} \dot{m}_i \cdot h_i = \sum_{outlet} \dot{m}_i \cdot h_i \quad (1)$$

The pumping, compression and expansion processes have been simulated considering a polytropic efficiency for the different turbomachinery of 90% (similarly to Ref. [48]), that leads to an isentropic turbine efficiency slightly higher than 90% and compressor one slightly lower than this value (as proposed in Ref. [47]). These processes are formulated as below:

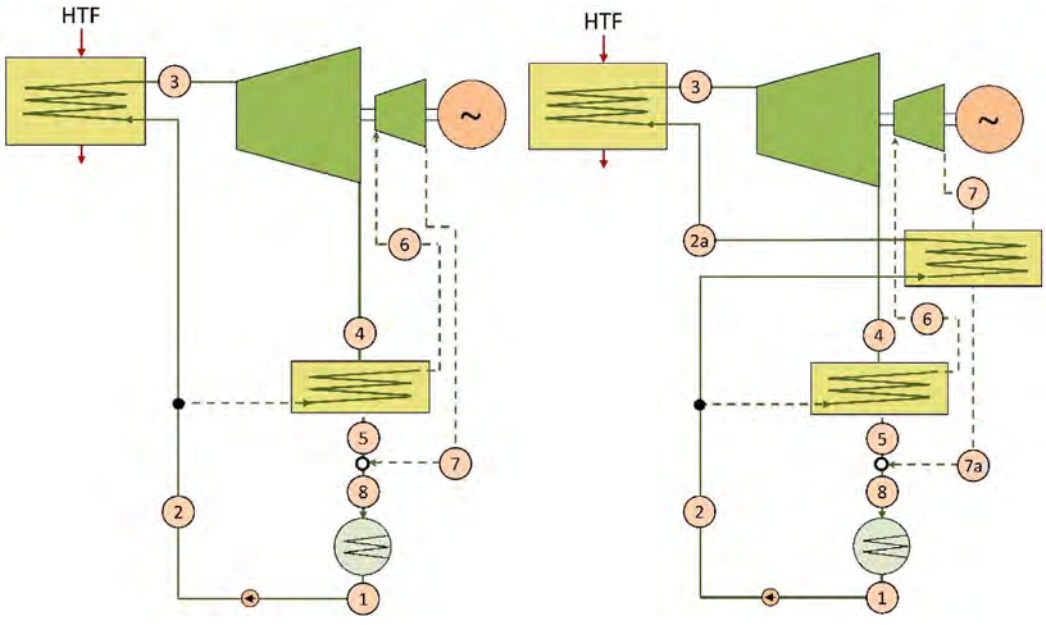

a) Single recuperated b) Double recuperated

Fig. 5. Layout of the RDE and DRDE cycles.

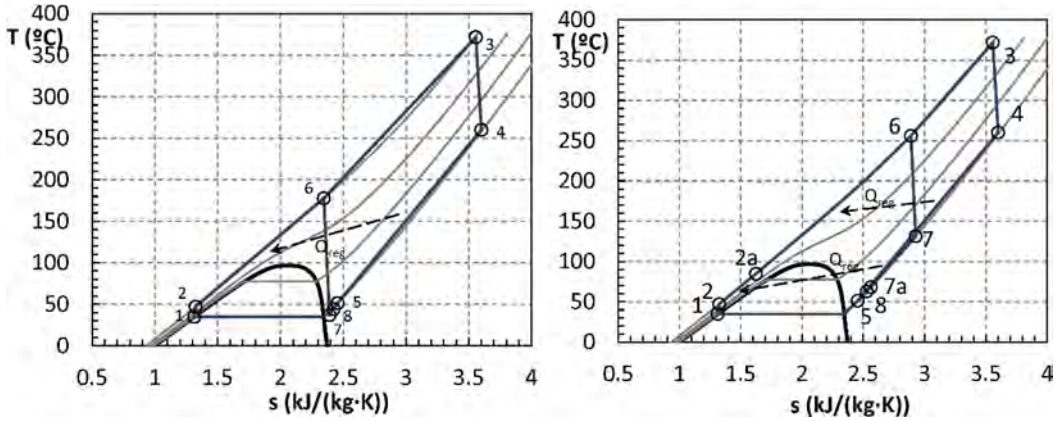

Fig. 6. Temperature-entropy diagram of the RDE and DRDR cycles.

$$\begin{cases} \delta h = \delta h_s/\eta_P = v\cdot\delta p/\eta_P \\ \delta h = \delta h_s/\eta_C = v\cdot\delta p/\eta_C \\ \delta h = \delta h_s\cdot\eta_T = v\cdot\delta p\cdot\eta_T \end{cases} \quad (3)$$

Due to the possible supercritical state of the working fluid and, thus, to the high variability of properties, particularly the specific heat, the numerical integration was carried out considering 20 steps between the inlet and outlet pressures in all cases.

Regarding the heat transfer processes, the pinch points in the heater and the recuperator were set to 5 °C [47]. Again, due to the supercritical nature of the fluid, the specific heat at constant pressure depends on temperature and pressure, so the pinch point in all heat exchangers were assessed calculating the corresponding temperature difference in 25 different sections along the heat exchanger.

The mass and energy balances, together with the definition of the design parameters and the mentioned technological parameters allows the complete simulation of the cycles. These parameters are summarised in Table 2.

The code of simulation model was developed in Visual Basic.

4.3. Figures of merit

As mentioned previously, from a thermodynamic point of view, the objective of a thermal power system should be to maximise energy conversion from the thermal energy available in the heat source to mechanical power:

Table 1
Maximum temperatures for the fluids, condensation pressure at 35 °C and references for properties.

Fluid	Maximum temperature	Condensation pressure at 35 °C	Reference
Ethanol	377 °C	0.14 bar	[41]
Propane	377 °C	12.2 bar	[39]
R11	352 °C	1.49 bar	[43]
Toluene	427 °C	0.062 bar	[42]
Water	Without limitation	0.056 bar	[40]

$$\dot{W} = \dot{m}_{HTF}\cdot c_{p,HTF}\cdot(T_{max,HTF} - T_{min,HTF})\cdot\eta \quad (4)$$

In the case of a closed heat source with fixed HTF temperature variation and thermal power supply, the maximisation of power leads to the maximisation of the thermal efficiency. Then, the figure of merit for application using closed heat sources can be the thermodynamic efficiency of the cycle:

$$\eta = (\sum \dot{m}_i\cdot w_T - \sum \dot{m}_i\cdot w_C - \sum \dot{m}_i\cdot w_P)/(\dot{m}_{heater}\cdot\Delta h_{heater}) \quad (5)$$

Besides, the exergy efficiency is the ratio of the power to the exergy transferred from the HTF to the working fluid:

$$\eta_\varepsilon = (\sum \dot{m}_i\cdot w_T - \sum \dot{m}_i\cdot w_C - \sum \dot{m}_i\cdot w_P)/(\dot{m}_{HTF}\cdot\Delta e_{HTF}) \quad (6)$$

However, in the case of an open thermal source (heat recovery), the thermodynamic efficiency of the cycle is not the only parameter to consider because the reduction of the HTF temperature to the lowest

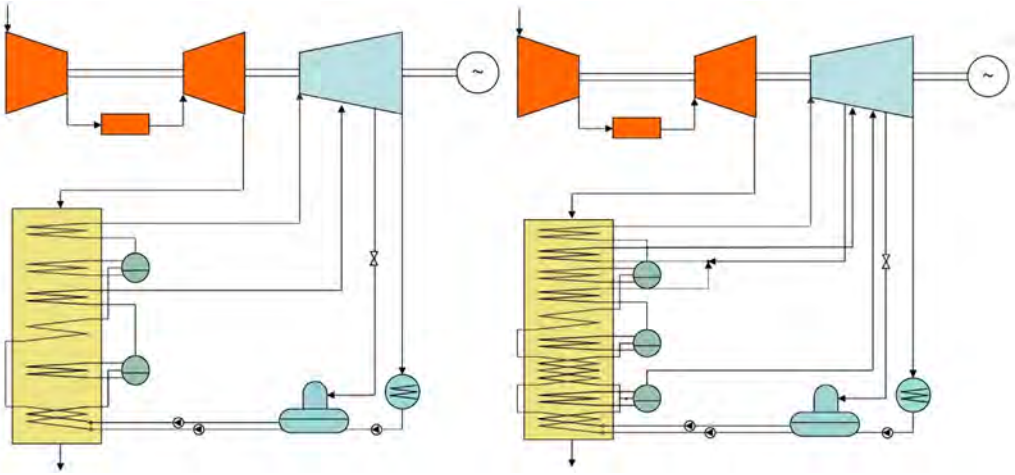

Fig. 7. Layout of 2P and 3P + R HRSGs (including the gas turbine and steam turbine).

Table 2
Design parameters and technological parameters.

Design parameters	
Maximum T of the HTF	400 °C (1st scenario), 300 °C (2nd scenario)
Minimum T of the HTF (closed sources)	290 °C (1st scenario), 190 °C (2nd scenario)
Ambient temperature	25 °C
Condensation temperature	35 °C
Pressure ratio	Variable
Balancing mass fraction	Variable
Secondary mass fraction	Variable
Technological parameters	
Polytropic efficiency of compressors (η_C)	90%
Polytropic efficiency of pumps (η_C)	90%
Polytropic efficiency of turbines (η_C)	90%
Pinch point in the heater	5 °C
Pinch points in the recuperators	5 °C
Approach points in subcritical HRSGs	5 °C
Pressure drop, high pressure isobar [48]	2%
Pressure drop, low pressure isobar [48]	5%

allowed value plays an important role. Therefore, the most adequate parameter to measure the performance in both cases is the exergy efficiency.

In this case, the exergy input is the exergy of the HTF coming from the heat source:

$$\eta_\varepsilon = (\sum \dot{m}_i \cdot w_T - \sum \dot{m}_i \cdot w_C - \sum \dot{m}_i \cdot w_P)/(\dot{m}_{HTF} \cdot e_{HTF}) \quad (7)$$

where e_{HTF} is the specific exergy of the HTF at the inlet of the heater.

Specific exergy is calculated as below:

$$e = (h - h_0) - T_0 \cdot (s - s_0) \quad (8)$$

In some circumstances the specific heat of the HTF can be considered as constant (i.e. molten salts). In this case, Eq. (7) can be simplified assuming null pressure drops:

$$e = c_p \cdot [(T - T_0) - T_0 \cdot ln(T/T_0)] \quad (9)$$

5. Results

5.1. Results of the HRB cycles in applications with fixed HTF temperature change.

As it was commented above, in applications with closed heat sources the maximum and minimum temperatures of the HTF are fixed. As the working fluid of the HRB cycle is selected, the parameters to be studied are the balancing mass fraction and the pressure ratio.

Fig. 8a and b show, respectively, the efficiencies of the HRB cycle for the two defined scenarios, considering different thermodynamic designs with different balancing mass fraction and pressure ratio. Performance of the reference cycles is also shown. As it is observed, the exergy efficiency of the HRB cycle increases as the pressure ratio (r) rises, approaching a maximum at a pressure ratio of about 14:1 for maximum HTF temperature of 400 °C (Fig. 8a) and about 10:1 for 300 °C (Fig. 8b). The corresponding heating pressures for these pressure ratios are 170 bar and 120 bar, respectively.

Besides, Fig. 8 shows that the efficiency increases with the balancing mass fraction, although results has been represented for balancing mass flows lower than those that exactly balance the recuperator. This analysis is completed with Fig. 9 that shows the thermal efficiency of the HRB cycle when the balancing mass flow is varied for different pressure ratios. As it is observed, for each pressure ratio, there is a change in the slope of the curves that corresponds with the design of completely balanced recuperator, and this point corresponds to the maximum exergy efficiency. Besides, Fig. 9b shows that at this point irreversibility is reduced at maximum, and that the trend is strongly influenced by the recuperator irreversibility.

Moreover, for a maximum HTF temperature of 400 °C (Fig. 8a), the HRB cycle reaches higher efficiencies than steam Rankine cycles (water 5-ext in Fig. 8) or ORCs, and it is reached at significantly lower pressure ratios (r). Particularly, efficiency of HRB is much higher than ORC's one using ethanol, and it is even higher than those reached by conventional water Rankine cycles and recuperative ORCs working with toluene, provided that the balancing mass rate is above a threshold placed roughly at 20%.

It is remarkable that conventional Rankine cycles are complex facilities due to the use of bleedings from the turbine to the regenerative preheaters and due to the low density of the steam at the final stages of the turbine and the condenser. Furthermore, the expansion ratio in the turbine is very high (usually above 2000:1), which leads to non-compact equipment. In the case of toluene, the facility is simpler than in the cases of Rankine and HRB cycles, although the efficiency is lower. Additionally, the expansion ratio in the expander is high (up to 500:1) and the condensation pressure low (about 0.06 bar for 35 °C, Table 1), which leads to non-compact equipment. Besides, there is the possibility of introduction of air inside the circuit (through the turbine seals or the condenser) due to the vacuum conditions, which becomes a risk due to the mixture of toluene and air.

Fig. 10 shows show the irreversibility breakdown for all the considered cycles for a maximum HTF temperature of 400 °C at the optimum pressure ratio (maximum efficiencies of Fig. 8a). As it is observed, the proposed HRB cycle reaches a reduced irreversibility in all the equipment avoiding components with large exergy losses, which

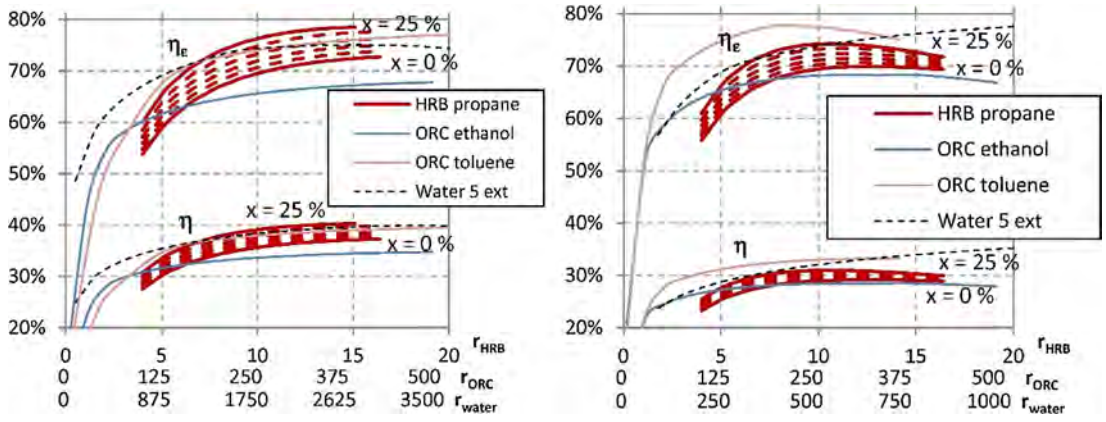

a) Maximum HTF temperature of 400 ºC b) Maximum HTF temperature of 300 ºC

Fig. 8. Efficiencies of the HRB and reference cycles.

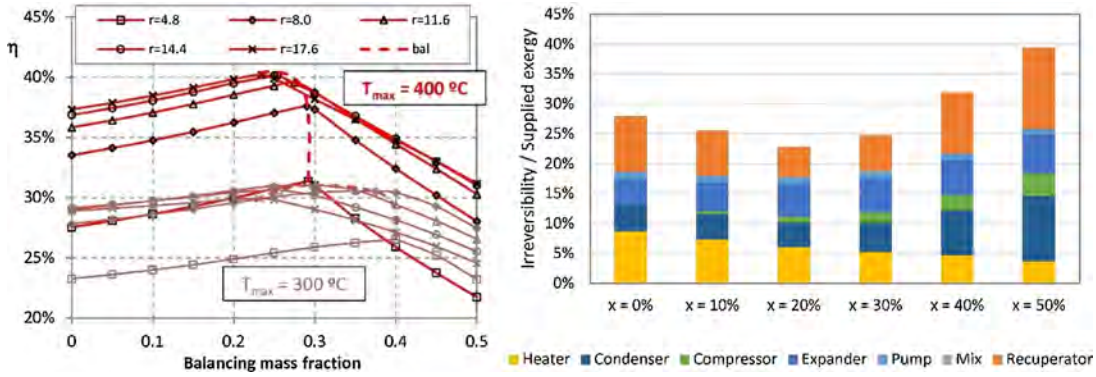

a) Efficiency b) Irreversibility (T_{max} = 400 ºC)

Fig. 9. Influence of the balancing mass fraction on the thermal efficiency and irreversibility of HRB cycle.

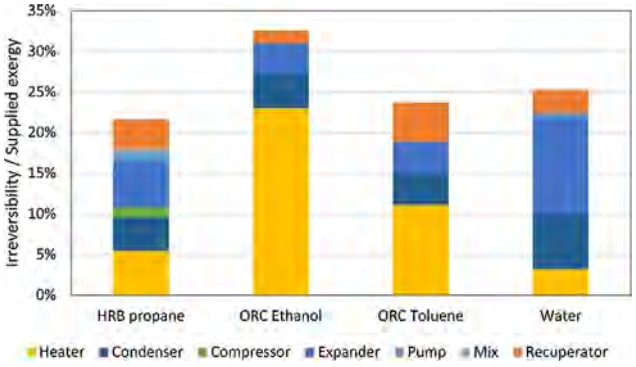

Fig. 10. Irreversibility for the considered cycles for closed heat sources.

Table 3
Representative points for a HRB cycle with maximum HTF temperature of 400 °C, pressure ratio of 14:1 and mass balancing mass fraction of 25%.

Point	$\dot{m}/\dot{m}_{heater}$	T (°C)	p (bar)	h (kJ/kg)	s (kJ/kg K)
1	0.75	35	12.1	292.4	1.313
2	0.75	47.1	170	328.2	1.324
3	0.75	258.4	170	994.9	2.904
4	1	243.6	170	945.3	2.809
5	1	377	166.5	1392.6	3.583
6	1	265.4	12.7	1149.4	3.626
7	1	53.4	12.1	649.4	2.469
8	0.25	199.8	170	796.2	2.508

make possible a high exergy efficiency for the whole plant.

For maximum HTF temperatures to 300 °C (Fig. 8b) the HRB cycle achieve higher exergy efficiency than the ethanol ORC but lower than the toluene ORC and conventional steam cycles with five steam bleedings.

On the other side, Fig. 11 shows the same series of results as in Fig. 8 but plotting the efficiency versus the temperature of the HTF exiting the heater. As it was commented, in this kind of applications, the minimum HTF temperature can be limited, and this can introduce important constraints to the cycle design. In each series the different lines represent the minimum possible HTF temperature as the pressure ratio of the cycle is modified. Therefore, the plotted temperature should be understood as precisely the minimum HTF temperature required by the cycle to operate with a pinch point of at least 5 °C. If the actual HTF minimum temperature is above this plotted limit, the cycle is suitable for the application. Thus, in the cases of the steam cycle and ORCs, every point in the plotted line corresponds to a different pressure ratio, which in turn leads to a cycle efficiency and a minimum HTF temperature that must be higher than the value that corresponds in abscissas. In the case of the HRB cycle, a set of curves are presented, each for a specific value of the balancing mass fraction.

This minimum HTF temperature was calculated assuming a pinch point of 5 °C in the heater (Section 3). It is important to highlight that due to the different nature of the cycles and the supercritical conditions of the fluids in some cases, the pinch point can be placed either at the hot-end of the heater, or at the-cold end or even delocalized, which avoid a clear trend for all cases.

For example, provided a maximum HTF temperature of 400 °C and a

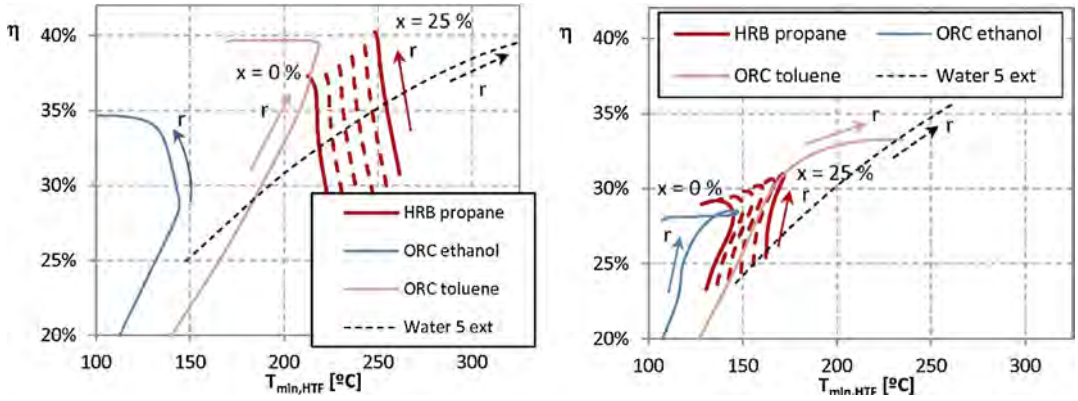

a) Maximum HTF temperature of 400 ºC b) Maximum HTF temperature of 300 ºC

Fig. 11. Efficiency vs minimum HTF temperature of HRB and reference cycles.

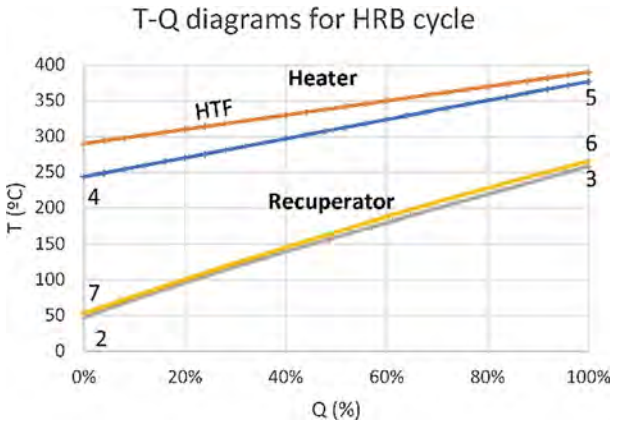

Fig. 12. Q-T diagram for the heater and recuperator of the HRB cycle.

limitation of the minimum HTF temperature of 290 °C, typical in conventional parabolic trough plants, Fig. 11 shows that the steam cycles with highest efficiency (around 38–40%) cannot be implemented, as they require higher minimum HTF temperatures than 290 °C, while all the HRB and ORC cycles can be used, and the highest efficiency is reached by the HRB cycle. If the limitation is set to 240 °C, which is close to the freezing point foreseen for future molten salts, not all the HRB designs are suitable but only those with balancing mass fractions below 20%. In this case, the most advisable choices, considering only the efficiency, are the HRB cycles and the ORC using toluene, while steam cycle designs have again limited performance. Finally, for minimum HTF temperatures of 200 °C and lower, the HRB cycle is not suitable, because the minimum HTF temperature is above 200 °C. Thus, this proposal is not advisable for heat recovery applications, since the exhaust temperature of the HTF that is required in this cycle is not low enough.

In the case of maximum HTF temperatures of 300 °C, the HRB cycle has better performance than water Rankine cycles, ethanol ORCs and toluene ORCs when the minimum HTF temperature ranges from 100 °C to 150 °C.

As an example, Table 3 shows the thermodynamic states of the representative points of a HRB cycle working with maximum HTF temperature of 400 °C, minimum HTF temperature of 290 °C, pressure ratio of 14:1 and balancing mass flow of 25%. In this case the pinch point within the heater is 23 °C (higher than 5 °C) due to the temperature limitation of propane (377 °C, far from the 400 °C of the HTF). The efficiency reached in this case is 40.1%.

Fig. 12 shows the Q-T diagrams for the same case of the HRB cycle of Table 3.

To sum up, the HRB cycle is a good candidate for finite heat sources, particularly with maximum HTF temperature around 400 °C. The performance is better than that reached by ORCs and conventional steam cycles and, due to the working pressure and pressure ratios, the equipment is expected to be more compact than using toluene or water, fluids that lead to efficiencies close to the maximum reached by the HRB cycle.

5.2. Results of the RDE cycles in applications of heat recovery.

As it has been discussed, the HRB cycle is not suitable for heat recovery applications due to the high minimum HTF temperature required. Conversely, heat recovery applications require low exhaust temperatures to recover as much thermal energy as possible. For that reason, some modifications to the HRB cycle were proposed that leads to the RDE cycle.

In a first step, the effect of the pressure ratio and the secondary mass fraction on the specific power of a RDE cycle using propane were investigated for two defined scenarios (maximum HTF temperatures of 400 °C and 300 °C, respectively).

Fig. 13 shows the exergy efficiency of the RDE cycle as the pressure ratio changes for different secondary mass fractions and the two scenarios. At low pressure ratios and low secondary mass fractions, the efficiency increases with increasing pressure ratios and increasing secondary mass fractions until a maximum. The optimum pressure ratio is higher at low secondary mass fractions and high maximum HTF temperatures.

The optimum secondary mass fraction is analysed with Fig. 14, which presents the exergy efficiency as the secondary mass flow changes for different pressure ratios and the same maximum HTF temperatures as before. Fig. 14 shows that the optimum secondary mass fraction is close to the balancing value in all cases, which takes place at the point where the slope of the curve changes. Fig. 14b shows that, at this point, the recuperator irreversibility is small despite the high mass fraction.

In a second step, the comparison of the RDE cycle with the reference ones was carried out. In the all cases the pressure ratio was optimized for each HTF maximum temperature, limiting the maximum pressure to 200 bar. For the RDE cycle, the secondary mass fraction was selected with the criterion of balancing the recuperator (equal temperature change in both streams, hot and cold). Both RDE and DRDE cycles were analysed, considering the type of configuration as another degree of freedom during the optimization process. For the ORCs (subcritical and transcritical) both non-recuperative and recuperative ORC were studied (again, the type of configuration is a degree of freedom), in the latter case, limiting the pinch points within the recuperator to 5 °C (as described in Section 3). Finally, for the 2P and 3P + R steam cycles, the approach points and the pinch points in the HRSG were set to 5 °C for all the pressure levels, and the high and intermediate pressure level were also optimised (the high pressure ones were also limited to 200 bar), while the low pressure level was set to 5 bar in both cases (2P

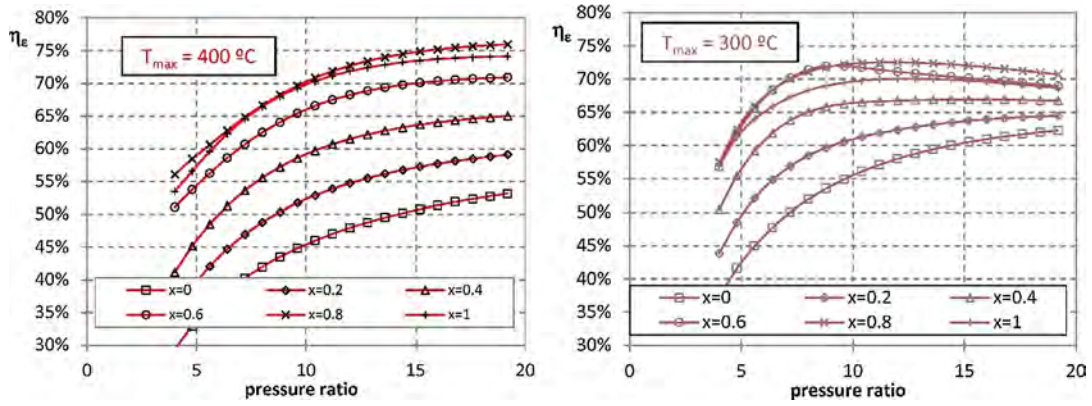

Fig. 13. Exergy efficiency of the RDE cycle.

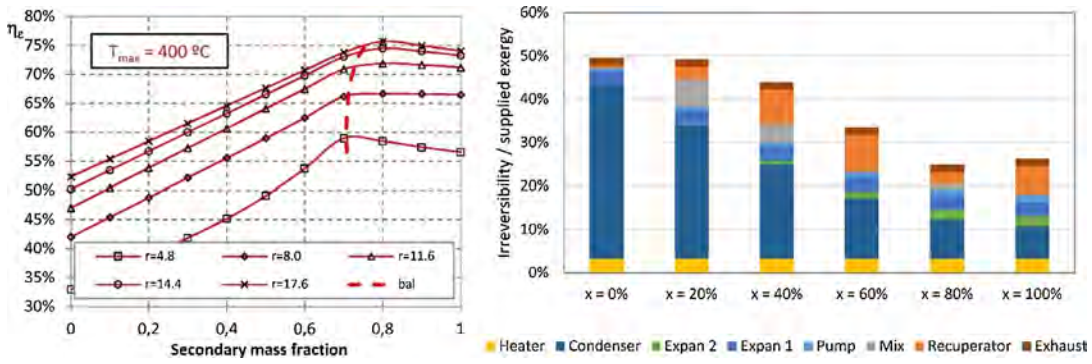

a) Exergy efficiency b) Irreversibility (T_{max} = 400 ºC)

Fig. 14. Influence of the secondary mass fraction on the exergy efficiency and irreversibility of the RDE cycle.

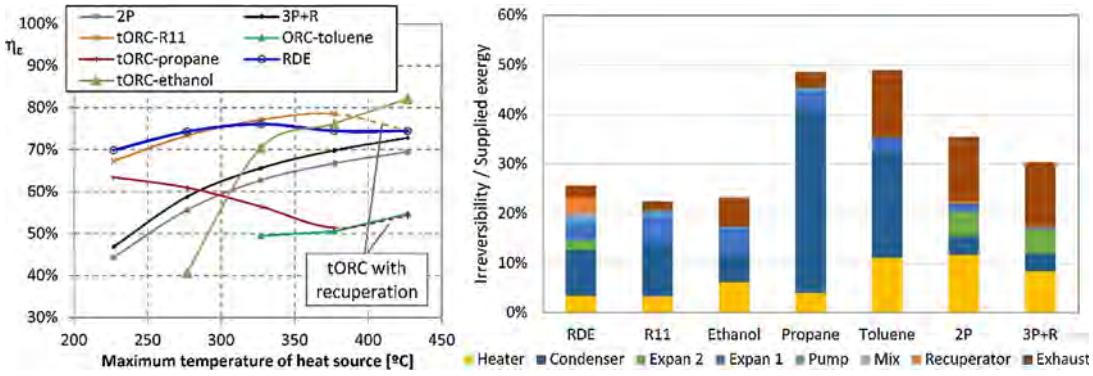

a) Exergy efficiency b) Irreversibility (T_{max} = 400 ºC)

Fig. 15. Exergy efficiency and irreversibility of the RDE and the reference cycles.

Table 4
Pressure levels, minimum temperature of the heat source, efficiency and secondary mass fraction for the RDE and reference cycles.

$T_{max,HTF}$ [°C]			227	277	327	377	427
Pressure [bar]	2P	HP	18.4	16.0	21.4	38.6	57.9
		LP	5.0	5.0	5.0	5.0	5.0
	3PR	HP	14.5	25.7	41.6	63.6	92.6
		IP	8.9	12.5	16.6	22.0	27.7
		LP	5.0	5.0	5.0	5.0	5.0
	tORC-R11		126.8	200.0	200.0	200.0	175.6*
	tORC-ethanol		–	62.9	200.0	200.0	200.0
	tORC-propane		175.7	200.0	200.0	200.0	200.0*
	ORC-toluene		11.5	24.3	7.3	13.6	40.1
	RDE		89.1	112.2	168.4	175.7	200
$T_{min,HTF}$ [°C]	2P		147.7	141.6	136.0	130.7	125.8
	3PR		147.7	141.8	136.4	131.5	127.0
	tORC-R11		34.9	52.8	63.8	50.3	84.8*
	tORC-ethanol		–	175.1	76.5	95.6	57.6
	tORC-propane		67.9	70.3	71.0	75.0	212.6*
	ORC-toluene		71.3	97.8	126.6	135.8	142.6
	RDE		59.9	59.7	65.8	68.9	56.0
Efficiency	2P		26.7%	28.5%	30.7%	32.4%	34.0%
	3PR		28.2%	30.2%	32.1%	34.0%	35.8%
	tORC-R11		16.8%	22.7%	27.4%	28.8%	32.1%*
	tORC-ethanol		–	25.3%	29.2%	32.5%	32.8%
	tORC-propane		19.1%	20.5%	20.6%	20.4%	37.3%*
	ORC-toluene		16.7%	24.4%	23.1%	25.1%	28.4%
	RDE		20.0%	23.7%	27.2%	28.9%	29.6%
x_{se}	RDE		66.7%	67.5%	73.6%	75.3%	76.6%

* Recuperative ORCs.

Table 5
Representative points for a RDE cycle with maximum HTF temperature of 400 °C, pressure ratio of 14:1 and mass balancing mass fraction of 25%.

Point	$\dot{m}/\dot{m}_{heater}$	T (°C)	p (bar)	h (kJ/kg)	s (kJ/kg K)
1	1.752	35	12.1	292.4	1.313
2	1.752	47.1	170	328.2	1.324
3	1	377	166.5	1392.6	3.583
4	1	265.4	12.7	1149.4	3.626
5	1	59.3	12.1	661.7	2.506
6	0.752	253.1	170	977.3	2.871
7	0.752	128.1	12.1	809.3	2.909
8	1.752	89.5	12.1	725.1	2.689

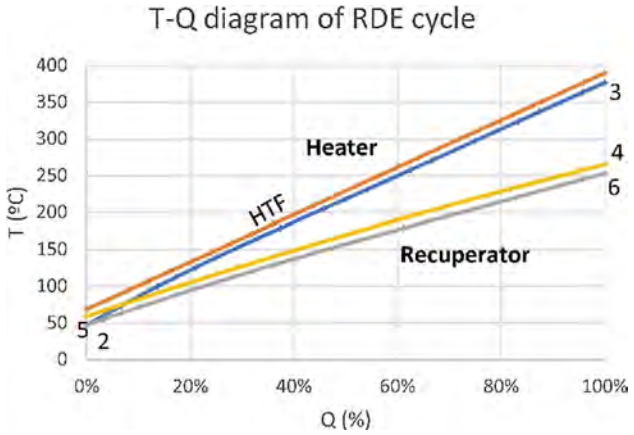

Fig. 16. Q-T diagram for the heater and recuperator of RDE cycle.

Table 6
Optimized parameters with minimum HTF temperature of 90 °C.

			$T_{max,HTF}$ [°C]				
			227	277	327	377	427
Pressure [bar]	2P	18.4	16.0	21.4	38.6	57.9	57.9
		5.0	5.0	5.0	5.0	5.0	5.0
	3PR	14.5	25.7	41.6	63.6	92.6	92.6
		8.9	12.5	16.6	22.0	27.7	27.7
		5.0	5.0	5.0	5.0	5.0	5.0
	tORC-R11		78.0	102.4	143.0*	159.4*	151.2*
	tORC-ethanol		–	62.9	178.3	200.0	113.4*
	tORC-propane		175.7*	200.0*	200.0*	200.0*	200.0*
	ORC-toluene		11.5	24.3	7.3	13.6	40.1
	RDE		112.2	144.0	144.0*	175.7*	200.0*
$T_{min,HTF}$ [°C]	2P		147.7	141.6	136.0	130.7	125.8
	3PR		147.7	141.8	136.4	131.5	127.0
	tORC-R11		90.0	90.5	91.1*	90.0*	90.9*
	tORC-ethanol		–	175.1	90.0	95.6	90.0*
	tORC-propane		90.2*	90.5*	90.6*	90.8*	200.1*
	ORC-toluene		90.0	90.0	90.0	103.7	92.3
	RDE		90.0	90.0	90.0*	100.8*	90.2*
Efficiency	2P		26.7%	28.5%	30.7%	32.4%	34.0%
	3PR		28.2%	30.2%	32.1%	34.0%	35.8%
	tORC-R11		18.5%	25.0%	29.9%*	32.5%*	32.7%*
	tORC-ethanol		–	27.7%	26.9%	32.4%	34.7%*
	tORC-propane		22.2%*	22.7%*	22.3%*	21.5%*	34.8%*
	ORC-toluene		16.7%	24.4%	23.1%	25.1%	28.4%
	RDE		20.1%	23.9%	28.2%*	32.2%*	32.6%*
x_{sec}	RDE		72.1%	72.4%	71.7%*	75.3%*	76.6%*

* Recuperative ORC or RDE with two recuperators.

and 3P + R).

Fig. 15 shows the results obtained for maximum HTF temperatures from 227 °C to 427 °C and the irreversibility breakdown for all cycles for a maximum temperature of the heat source of 400 °C, while Table 4 shows the value of the optimized pressures, the exhaust temperature of the HTF, the efficiency of the cycle and the secondary mass fraction for the RDE cycle.

Results show that the RDE cycle achieves good performance for the range of temperature considered (and that the DRDE cycle is not advisable) and low irreversibility in all the equipment. Only transcritical ORCs using R11 and ethanol can compete with the RDE cycle performance or improve it because these fluids implement quasi-triangular or trilateral thermodynamic cycles. In fact, the DRE cycle, thanks to the well balanced recuperator, can be understood as equivalent to a trilateral cycle despite the superheated state at the exit of the expander, because the heat corresponding to the de-superheating process in the recuperator is used to obtain additional power without affecting the temperature at the heater inlet. Moreover, in Fig. 15b one can observe that the irreversibility of trilateral cycles (R11 and ethanol) are very similar to DRE's, which is slightly higher due to the recuperator one. In these cases, the advantage of the RDE cycle is the use of a more favourable fluid. In fact, R11 is a forbidden fluid. Regarding ethanol, its condensation pressure is below the ambient pressure (Table 1), which convey potential risk of air introduction.

Transcritical ORCs using propane, subcritical ORCs using toluene and steam cycles using 2P and 3P + R heat recovery steam generators cannot reach as much exergy efficiency as the RDE cycle.

For temperatures higher than 423 °C, 2P and 3P + R steam cycles become the best (not represented in the figure). These results indicate the favourable behaviour of the RDE cycle until the working fluid (propane) reaches the maximum allowed temperature (377 °C). From there, RDE cycle cannot get benefit from the high temperature of the HTF and it begins to loss its advantage in favour of the steam cycles.

As an example, Table 5 shows the thermodynamic states of the representative points of a RDE cycle working with maximum HTF temperature of 400 °C, pressure ratio of 14:1 and balanced secondary mass flow. For a pinch point in the heater of 5 °C, the minimum HTF temperature is 59.2 °C. As the temperature differences at the hot- and cold-end of the heater are 23 °C and 12.1, respectively, the pinch point is reached in an intermediate position of the heat exchanger. The same circumstance occurs in the recuperator, where the temperature differences at the hot- and cold-end are 12.3 °C and 12.2 °C, respectively, while the pinch point is 5 °C. The secondary mass fraction is 0.752, which allows a well-balanced recuperator with quite similar temperature differences at both hot- and cold-ends. The thermal efficiency in this case is 28.8% (a low value because it is not optimised) and the exergy efficiency of 74.3%.

Fig. 16 shows the Q-T diagrams for the RDE cycle shown in table 5.

Finally, the same analysis was repeated considering a slight limitation of the HTF temperature of 90 °C at the exit of the heater (typical to avoid acid dew points). Table 6 summarizes the results. As it was expected, the exergy efficiency is lower and, due to the minimum HTF limitation, the recuperative cycles become the best option in more cases than before (including the DRDE configuration). Despite these differences, in all cases the trends are the same for all fluids and cycles.

To sum up, the RDE cycle exhibits good performance for heat recovery using sources from moderate to high temperatures (200–400 °C) and this performance is limited at higher HTF temperatures due to the temperature limitation imposed to working fluid of the cycle.

6. Conclusions

The paper presents and studies two thermodynamic cycles designed to work with finite heat sources, which are particularly suitable for maximum temperatures of about 400 °C. One of them, namely the HRB cycle, is aimed to work with open heat sources having limited temperature variation (i.e. solar thermal power plants). The other one, namely the RDE cycle, is based on the HRB but introduces some modifications to work in heat recovery applications or open heat sources. Regarding the closed heat sources, the HRB cycle using propane as

working fluid presents higher exergy efficiency than ORCs and conventional steam cycles. The efficiency increase over ORCs is significant. When it is compared with conventional steam cycles and toluene ORC, the efficiency increase is lower, but HRB cycle should also lead to more compact equipment (for example, condenser and expander do not work at vacuum conditions and the expansion ratio is lower). These features make the HRB cycle a good candidate for this kind of heat sources, particularly at the temperature range of 400 °C.

Regarding the open heat sources, for temperatures up to 400 °C, the RDE cycle using propane allows higher exergy efficiency than conventional Rankine cycles with conventional heat recovery steam generators of two and three pressure levels, and better than some subcritical and transcritical ORCs. Only transcritical ORCs that configure quasi-triangular or trilateral cycles (for example, using R11 or ethanol) reach or even improve the performance over the RDE cycle, but the latter allows the use of a more favourable fluid (propane).

Future works should involve aspects like the study of the cycles in specific sites, the design of the different equipment (turbomachinery and heat exchangers, particularly the recuperators that can be very large) and the yearly operation of the systems or the analysis of the power plant behaviour under real operation scenarios. Additionally, economic aspects should also be addressed as well as the prospection of different fluids or the study of the fluid degradation at the working conditions to investigate the extension of the good performance toward higher temperatures.

CRediT authorship contribution statement

Antonio Rovira: Conceptualization, Methodology, Software, Writing - original draft, Visualization, Supervision, Funding acquisition. **Marta Muñoz:** Methodology, Validation, Writing - review & editing. **Consuelo Sánchez:** Methodology, Writing - review & editing. **Rubén Barbero:** Software, Visualization.

Declaration of Competing Interest

The authors declare that they have no known competing financial interests or personal relationships that could have appeared to influence the work reported in this paper.

Acknowledgments

This work has been supported by the Spanish Ministry of Economy and Competitiveness through the ENE2015-70515-C2-1-R project.

Appendix A. Supplementary material

Supplementary data to this article can be found online at https://doi.org/10.1016/j.applthermaleng.2019.114805.

References

[1] H. Zhai, et al., Categorization and analysis of heat sources for organic Rankine cycle systems, Renew. Sustain. Energy Rev. 64 (2016) 790–805 10.1016/j.rser.2016.06.076.
[2] H. Chen, D.Y. Goswami, E.K. Stefanakos, A review of thermodynamic cycles and working fluids for the conversion of low-grade heat, Renew. Sustain. Energy Rev. 14 (9) (2010) 3059–3067, https://doi.org/10.1016/j.rser.2010.07.006.
[3] S.C. Yu, L. Chen, Y. Zhao, H.X. Li, X.R. Zhang, Thermodynamic analysis of representative power generation cycles for low-to-medium temperature applications, Int. J. Energy Res. 39 (2015) 84–97, https://doi.org/10.1002/er.3221.
[4] K. Braimakis, S. Karellas, Integrated thermoeconomic optimization of standard and regenerative ORC for different heat source types and capacities, Energy 121 (2017) 570–598, https://doi.org/10.1016/j.energy.2017.01.042.
[5] B.F. Tchanche, et al., Low-grade heat conversion into power using organic Rankine cycles: a review of various applications, Renew Sustain. Energy Rev 15 (2011) 3963–3979, https://doi.org/10.1016/j.rser.2011.07.024.
[6] A. Rovira, C. Rubbia, M. Valdés, J.M. Martínez-Val, Thermodynamic cycles optimised for medium enthalpy units of concentrating solar power, Energy 67 (2014) 176–185, https://doi.org/10.1016/j.energy.2014.02.029.
[7] D. Sánchez, B. Monje Brenes, J.M. Muñoz de Escalona, R. Chacartegui, Non-conventional combined cycle for intermediate temperature systems, Int. J. Energy Res. 37 (2013) 403–411, https://doi.org/10.1002/er.2945.
[8] H. Singh, R.S. Mishra, Performance evaluation of the supercritical Organic Rankine Cycle (SORC) integrated with large scale solar parabolic trough collector (SPTC), System: Exergy Energy Anal. Environ. Progr. Sustain. Energy 37 (2) (2018) DOI 10.1002/ep.
[9] H.U. Helvaci, Z.A. Khan, Thermodynamic modelling and analysis of a solar organic Rankine cycle employing thermofluids, Energy Convers. Manage. 138 (2017) 493–510, https://doi.org/10.1016/j.enconman.2017.02.011.
[10] P.J. Yekoladio, T. Bello-Ochende, J.P. Meyer, Thermodynamic analysis and performance optimization of organic Rankine cycles for the conversion of low-to moderate grade geothermal heat, Int. J. Energy Res. 39 (2015) 1256–1271, https://doi.org/10.1002/er.3326.
[11] S. Lecompt, et al., Review of organic Rankine cycle (ORC) architectures for waste heat recovery, Renew. Sustain. Energy Rev. 47 (2015) 448–461, https://doi.org/10.1016/j.rser.2015.03.089.
[12] Zhao M, Xu F, Wei M Tian G, Zhang H. Simulation analysis of cooling methods of an on-board organic Rankine cycle exhaust heat recovery system. Int J Energy Res. 2017;41:2480–2490. https://doi.org/10.1002/er.3809.
[13] M. Gleinser, Ch. Wieland, The Misselhorn cycle: batch-evaporation process for efficient low-temperature waste heat recovery, Energies 9 (2016) 337, https://doi.org/10.3390/en9050337.
[14] M. Gleinser, Ch. Wieland, H. Spliethoff, Batch evaporation power cycle: influence of thermal inertia and residence time, Energy 157 (2018) 1090–1101, https://doi.org/10.1016/j.energy.2018.05.145.
[15] G. Angelino, C. Invernizzi, Real gas Brayton cycles for organic working fluids, Proc. IMechE Part A J. Power Energy 215 (2001) 27–37.
[16] A. Rovira, J. Muñoz-Antón, M.J. Montes, J.M. Martínez-Val, Optimization of Brayton cycles for low-to-moderate grade thermal energy sources, Energy 55 (2013) 403–416, https://doi.org/10.1016/j.energy.2013.03.094.
[17] P.D. Malali, S.K. Chaturvedi, T. Abdel-Salam, Performance optimization of a regenerative Brayton heat engine coupled with a parabolic dish solar collector, Energy Convers. Manage. 143 (2017) 85–95, https://doi.org/10.1016/j.enconman.2017.03.067.
[18] M.R. Meas, T. Bello-Ochende, Thermodynamic design optimisation of an open air recuperative twin-shaft solar thermal Brayton cycle with combined or exclusive reheating and intercooling, Energy Convers. Manage. 148 (2017) 770–784, https://doi.org/10.1016/j.enconman.2017.06.043.
[19] M. Saghafifar, M. Gadalla, A critical assessment of thermo-economic analyses of different air bottoming cycles for waste heat recovery, Int. J. Energy Res. (2018) 1–27, https://doi.org/10.1002/er.4243.
[20] J. Muñoz-Antón, C. Rubbia, A. Rovira, J.M. Martínez-Val, Performance study of solar power plants with CO_2 as working fluid. A promising design window, Energy Convers. Manage. 92 (2015) 36–46, https://doi.org/10.1016/j.enconman.2014.12.030.
[21] K. Brun, P. Friedman, R. Dennis, Fundamentals and Applications of Supercritical Carbon Dioxide (sCO_2) Based Power Cycles, Elsevier, Waltham MA, 2017.
[22] P. Kumar, K. Srinivasan, Carbon dioxide based power generation in renewable energy systems, Appl. Therm. Eng. 109 (2016) 831–840, https://doi.org/10.1016/j.applthermaleng.2016.06.082.
[23] M.A. Reyes-Belmonte, A. Sebastián, M. Romero, J. González-Aguilar, Optimization of a recompression supercritical carbon dioxide cycle for an innovative central receiver solar power plant, Energy 112 (2016) 17–27, https://doi.org/10.1016/j.energy.2016.06.013.
[24] M. Binotti, et al., Preliminary assessment of sCO2 cycles for power generation in CSP solar tower plants, Appl. Energy 204 (2017) 1007–1017, https://doi.org/10.1016/j.apenergy.2017.05.121.
[25] L. Coco-Enríquez, J. Muñoz-Antón, J.M. Martínez-Val, Dual Loop line-focusing solar power plants with supercritical Brayton power cycles, Int. J. Hydrogen Energy 42 (2017) 17664–17680, https://doi.org/10.1016/j.ijhydene.2016.12.128.
[26] K. Wang, Y.L. He, Thermodynamic analysis and optimization of a molten salt solar power tower integrated with a recompression supercritical CO_2 Brayton cycle based on integrated modeling, Energy Convers. Manage. 135 (2017) 336–350, https://doi.org/10.1016/j.enconman.2016.12.085.
[27] J.I. Linares, et al., Recuperated versus single-recuperator re-compressed supercritical CO_2 Brayton power cycles for DEMO fusion reactor based on dual coolant lithium lead blanket, Energy 140 (2017) 307–317, https://doi.org/10.1016/j.energy.2017.08.105.
[28] L. Vesely, V. Dostal, S. Entler, Study of the cooling systems with S-CO_2 for the DEMO fusion power reactor, Fusion Eng. Des. 124 (2017) 244–247, https://doi.org/10.1016/j.fusengdes.2017.05.029.
[29] S. Hou, Y. Wu, Y. Zhou, L. Yu, Performance analysis of the combined supercritical CO2 recompression and regenerative cycle used in waste heat recovery of marine gas turbine, Energy Convers. Manage. 151 (2017) 73–85, https://doi.org/10.1016/j.enconman.2017.08.082.
[30] M.J. Li, et al., The development technology and applications of supercritical CO2 power cycle in nuclear energy, solar energy and other energy industries, Appl. Therm. Eng. 126 (2017) 255–275, https://doi.org/10.1016/j.applthermaleng.2017.07.173.
[31] G. Demirkaya, et al., Thermal and exergetic analysis of the goswami cycle integrated with mid-grade heat sources, Entropy 19 (2017) 416, https://doi.org/10.3390/e19080416.
[32] X. Li, A trapezoidal cycle with theoretical model based on organic Rankine cycle, Int. J. Energy Res. 40 (2016) 1624–1637, https://doi.org/10.1002/er.3528.
[33] Y.M. Kim, C.G. Kim, D. Favrat, Transcritical or supercritical CO_2 cycles using both

low- and high-temperature heat sources, Energy 43 (2012) 402–415, https://doi.org/10.1016/j.energy.2012.03.076.
[34] D.M. Cakici, A. Erdogan, C.O. Colpan, Thermodynamic performance assessment of an integrated geothermal powered supercritical regenerative organic Rankine cycle and parabolic trough solar collectors, Energy 120 (2017) 306–319, https://doi.org/10.1016/j.energy.2016.11.083.
[35] P.X. Jiang, F.Z. Zhang, R.N. Xu, Thermodynamic analysis of a solar–enhanced geothermal hybrid power plant using CO_2 as working fluid, Appl. Therm. Eng. 116 (2017) 463–472, https://doi.org/10.1016/j.applthermaleng.2016.12.086.
[36] E. Bellos, C. Tzivanidis, Investigation of a hybrid ORC driven by waste heat and solar energy, Energy Convers. Manage. 156 (2018) 427–439, https://doi.org/10.1016/j.enconman.2017.11.058.
[37] A.M. Pantaleo, et al., Novel hybrid CSP-biomass CHP for flexible generation: Thermo-economic analysis and profitability assessment, Appl. Energy 204 (2017) 994–1006, https://doi.org/10.1016/j.apenergy.2017.05.019.
[38] A.M. Pantaleo, et al., Hybrid solar-biomass combined Brayton/organic Rankine-cycle plants integrated with thermal storage: techno-economic feasibility in selected Mediterranean areas, Renew. Energy (2018), https://doi.org/10.1016/j.renene.2018.08.022.
[39] A. Rovira, M. Muñoz, C. Sánchez, J.M. Martínez-Val, Proposal and study of a balanced hybrid Rankine-Brayton cycle for low-to-moderate temperature solar power plants, Energy 89 (2015) 305–317, https://doi.org/10.1016/j.energy.2015.05.128.
[40] Bombarda P, Gaia M, Invernizzi C, Pietra C. Comparison of Enhanced Organic Rankine Cycles for Geothermal Power Units. Proceedings World Geothermal Congress 2015. Melbourne, Australia, 19-25 April 2015.
[41] Rovira A. Muñoz, Montes M.J. Sánchez, Off-design analysis of a Hybrid Rankine-Brayton cycle used as the power block of a solar thermal power plant, Energy 134 (2017) 369–381, https://doi.org/10.1016/j.energy.2017.06.014.
[42] E.W. Lemmon, M.O. McLinden, W. Wagner, Thermodynamic properties of propane. III. A reference equation of state for temperatures from the melting line to 650 K and pressures up to 1000 MPa, J. Chem. Eng. Data 54 (2009) 3141–3180.
[43] W. Wagner, A. Pruss, The IAPWS formulation 1995 for the thermodynamic properties of ordinary water substance for general and scientific use, J. Phys. Chem. Ref. Data 31 (2) (2002) 387–535.
[44] E.W. Lemmon, R. Span, Short fundamental equations of state for 20 industrial fluids, J. Chem. Eng. Data 51 (2006) 785–850.
[45] H.E. Dillon, S.G. Penoncello, A fundamental equation for calculation of the thermodynamic properties of ethanol, Int. J. Thermophys. 25 (2) (2004) 321–335.
[46] R.T. Jacobsen, S.G. Penoncello, E.W. Lemmon, A fundamental equation for trichlorofluoromethane (R-11), Fluid Phase Equilib. 80 (1992) 45–56.
[47] R.V. Padilla, Y.C. Soo Too, R. Benito, W. Stein, Exergetic analysis of supercritical CO_2 Brayton cycles integrated with solar central receivers, Appl. Energy 148 (2015) 348–365, https://doi.org/10.1016/j.apenergy.2015.03.090.
[48] M. Binotti, M. Astolfi, S. Campanari, G. Manzolini, P. Silva, Preliminary assessment of sCO2 cycles for power generation in CSP solar tower plants, Appl. Energy 204 (2017) 1007–1017, https://doi.org/10.1016/j.apenergy.2017.05.121.